Geol Survey

Mineralogy and Diagenesis of the Pennsylvanian Browning Sandstone on the Western Shelf of the Illinois Basin

Duane M. Moore

Cover photo: Three feet of loess overlies an outcrop of the Pennsylvanian Browning Sandstone in the east bank of Wilson Creek in the Beardstown Quadrangle.

Mineralogy and Diagenesis of the Pennsylvanian Browning Sandstone on the Western Shelf of the Illinois Basin

Duane M. Moore

CONTENTS

ABSTRACT

The clay minerals, micas, and feldspars of the Pennsylvanian (Desmoinesian) Browning Sandstone indicate that significant diagenetic changes, with accompanying exchanges, removals, and additions of material, have occurred in this unit. Independent evidence indicates that these rocks have experienced maximum burial of ≤1 km on the Western Shelf of the Illinois Basin and were never heated to more than ~60°C, except for a very brief thermal pulse that may have raised the temperature to ≤80°C. Illite smectite (I/S) in the Browning Sandstone is equal to or ≥90% illite. The chemical compositions of 0.09- to 0.063-mm feldspar grains from this unit are not similar to modern detrital suites of feldspars. Although the feldspar compositions are similar to diagenetic sequences described by others from greater burial depths, they are somewhat different from the diagenetically altered feldspar assemblage in the Purington Shale, which is in the same cyclothem as the Browning Sandstone. The simplest interpretation of the apparently advanced stage of diagenesis, which is comparable with that of more deeply buried Cenozoic and Mesozoic sediments from similar depositional environments, is that the diagenetic processes have been operating at less intensity but for a longer time at significantly lower temperatures. This phenomenon is an example of low-temperature, time-dependent diagenesis, which apparently prevails throughout the Illinois Basin.

INTRODUCTION

Little has been published comparing the diagenetic histories of cratonic basins with those of deep marginal basins such as the Gulf of Mexico Basin. Both types of basins may have similar source areas, but quite different rates of subsidence. More rapid rates of subsidence apparently lead to deeper burial, higher temperatures, and, therefore, more advanced stages of diagenesis. Hower and Altaner (1983) and Grathoff and Moore (1996), among others, called attention to the apparently advanced stage of diagenesis exhibited by Paleozoic shales and bentonites of the Illinois Basin. It seems anomalous that the diagenetic stage of the Browning Sandstone apparently is the same as that of Cenozoic and Mesozoic sediments (e.g., the Gulf Coast Basin), which have been at significantly greater depths and higher temperatures.

Understanding how much and in what ways sediments change physically and chemically in the process of becoming rock remains an unfinished puzzle. Contributing to the puzzle's complexity are the different patterns of diagenesis that have been noted for different basins (Primmer and Shaw 1985, de Caritat et al. 1997, Lanson et al. 1998). Changes in sandstones seem to be somewhat better understood than those in shales for two reasons: (1) the larger grain size and generally simpler mineralogy of sandstones makes them easier to study, and (2) their perceived greater economic importance as reservoirs and aquifers has encouraged more research. Studies of diagenesis in clastic units have examined both geochemical and mineralogical changes. Significant chemical and physical changes can be tracked in the clay-size fraction and in framework grains. The primary method of tracking change in the former is the transformation of smectite to illite as a measure of maturity (Perry and Hower 1970, Hower et al. 1976, Gharrabi and Velde 1995, Lynch 1997). In addition, a recently described method is the transformation of an Fe-rich 7Å clay mineral to chlorite with a related change in the polytype of the chlorite (Ryan and Reynolds 1996, Ryan et al. 1998). This serpentine/chlorite mixed-layered clay mineral also was reported in Mississippian siliciclastic reservoirs in the

Illinois Basin (Moore and Hughes 1991). Among the framework grains, changes of feldspars and micas have received detailed attention (Land and Milliken 1981; Milliken 1988, 1992; Milliken et al. 1989; Land et al. 1997; Moore 2000). Feldspars change in their post-burial environments from the wide variety of compositions one would associate with a modern detrital assemblage to assemblages dominated by albite (for example, Land and Milliken 1981, Boles 1982) and, in some places, by albite and K-feldspar (Land et al. 1997).

As part of a study of sandstone and shale of the Liverpool cyclothem in western Illinois (fig. 1) (Moore 1978, 1982, 1984, 2000), this report offers a tabulation of chemical compositions of feldspars and micas and an identification of the clay minerals for a Pennsylvanian age sandstone from the Western Shelf of the cratonic Illinois Basin, with special attention to the illitic clay minerals. These data indicate that this unit has reached a stage of diagenesis similar to that of younger sediments of similar composition, but at greater depths and higher temperatures. Because the Browning Sandstone is recognized only in western Illinois (Wright 1966, Willman et al. 1975), tracking changes by depth of burial cannot be done. However, compared with samples of the Purington Shale (fig. 1) and shales of the Ordovician Maquoketa Group (Grathoff 1996), the clay minerals of the Browning Sandstone have approximately the same maturity as clay minerals from the deepest parts of the Illinois Basin. Therefore, the Browning Sandstone is presented as an example of a unit that has undergone low-temperature, time-dependent diagenesis.

In addition to providing insight into diagenetic history, the mineralogy of siliciclastic units is used to judge the quality of reservoirs for oil and gas, to judge their usefulness as aquifers, and to interpret the tectonic style of their source areas(s). An understanding of diagenetic changes is essential for accurate interpretations of the origins of the units of shallow Paleozoic basins worldwide.

GEOLOGIC SETTING

The geologic setting for the Browning Sandstone is the Illinois Basin, a mature, petroleum-producing, interior cratonic basin (Leighton et al. 1990). The Browning Sandstone is a member of the Tradewater Formation (Greb et al. 1992) and is the basal sandstone of the Liverpool cyclothem (fig. 1).
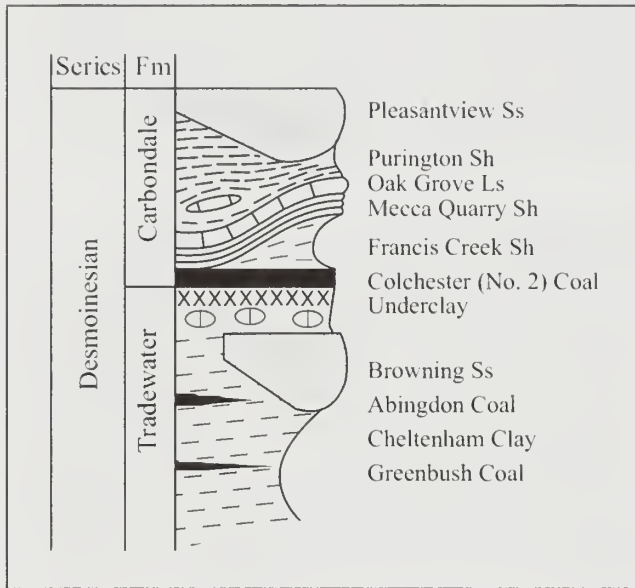
The Browning Sandstone occurs as channel and sheet facies that commonly grade to siltstone or silty shale within short distances (Wright 1966, Willman et al. 1975). This member is named from exposures in Sec. 18, T2N, R1E, Beardstown Quadrangle, Schuyler Co., Illinois (Wanless 1957). The type section of the Browning Sandstone is an outcrop of a massive lens topped by flaggy sandstone that rises about 3 m above the water level of a small stream. It has probably never been buried more than about 1 km (and probably somewhat less) or heated to more than about 60°C (Hacquebard 1977, Harvey et al. 1977, Bostick et al. 1979, Cluff and Byrnes 1990, Damberger 1991), except for an approximately 200,000-year thermal pulse that may have raised temperatures of the Browning Sandstone to as much as 80°C (Rowan and Goldhaber 1996). As has been argued in detail by Moore (2000), heat would have been conducted through the approximately 555 m between the Ordovician and Cambrian fluid-carrying units and the Browning Sandstone. During conduction, the temperature at the front of the heat pulse would have decreased to not more than 20 to 25% of the difference in temperatures between the source and the Browning Sandstone. Additionally, the Browning Sandstone would have been exposed to these increased temperatures for perhaps 10% of the overall time of the thermal pulse in the Ordovician and Cambrian rocks.

Moore (2000) reported on the diagenetic character of the Purington Shale, which lies just a few units above the Browning Sandstone (fig. 1) in the same cyclothem. Little other work has been reported on this unit.

Figure 1 Stratigraphic relationships of the Browning Sandstone and the Purington Shale members of the Liverpool Cyclothem, which goes from the base of the Browning Sandstone to the base of the Pleasantville Sandstone.

METHODS

Browning Sandstone samples were collected from the type section (Wanless 1957) and from outcrops along Cedar Fork Creek in Sec. 14 and 23, T9N, R1W, Abingdon Quadrangle, southeastern Warren Co., Illinois. Separation of the 0.09- to 0.0625-mm (3.5- to 4-ϕ size) feldspar and mica grains and preparation of the suspensions for studying the clay minerals were two separate operations.

To prepare mounts for examination with the microprobe, about 1.5 kg of sample material was gently crushed, soaked overnight, sonified to disaggregate the rock, and then screened, quartered, and sorted. The material was washed through 0.25-, 0.09-, and 0.063-mm screens. The residues were dried at 100°C and run through a magnetic separator at least three times to remove magnetically susceptible mineral grains. A binocular microscope was used to hand-pick feldspar and mica grains from the 0.09- to 0.0625-mm fraction yielded by this process. In an attempt to avoid bias, a cleaned aliquot was divided into fourths, placed one in a watch glass, and tried to pick out all feldspar and mica grains, placing them in separate containers. Then the collected feldspars and micas were each quartered, and one

quarter was selected as the portion to mount for microprobe analysis. Grains were suspended in epoxy, ground to a flat surface, and mounted as thin sections. Throughout, chemical treatments were avoided. A few quartz and chlorite grains were included accidentally, but, when microprobed, their analyses were easily detected.

The feldspar and mica grains were analyzed using the microprobe and associated programs for analysis in the laboratory of J.V. Smith at the University of Chicago. Standards of this laboratory included asb microcline (no. 76), Amelia albite (no. 75), plag An 60 (no. 82), diopside glass (no. 73), V glass (no. 89), and Kakanui hornblende (no. 99). The microprobe used a wavelength dispersive system. Using these standards, feldspar and mica grains were analyzed for Al, Ca, Fe, K, Na, and Si. In addition, mica grains were analyzed for Cr, Mg, Mn, and Ti. In a second series of analyses, also using a wavelength dispersive system, feldspar grains were tested for Ba, Fe, Mg, Rb, and Sr. Analytical conditions for the analysis of feldspar grains were 10 nA, 15 kV, counting times of 54.0 to 54.5 seconds, and a beam diameter of 10 μm. For mica grains, the analytical

conditions were the same, except that the beam current was 20 nA. As tests of precision, one feldspar grain was probed 9 times, and one mica grain was probed 10 times.

Identification of clay minerals in the Browning Sandstone by x-ray diffraction (XRD) analysis was made on oriented aggregates. Samples were prepared by sonifying, centrifuging, and then sedimenting on glass slides (Moore and Reynolds 1997). After drying, after glyceolation, and again after heating, the samples were exposed to CuKα radiation in a Scintag* theta-theta diffractometer. NEWMOD* was used (Reynolds 1985) to aid in identification of the clay minerals from the oriented aggregates. To determine a quantitatively representative modal analysis, the relative intensity ratios (RIR) of Hughes et al. (1994) was used.

The method of Grathoff and Moore (1996) was used to prepare randomly oriented powders of samples and to measure quantities of illite polytypes. For the $2M_1$ polytype, the integrated intensity (area) from the (025) and (11$\bar{6}$) peaks at 29.9° and 32.1°2θ, respectively (fig. 2), agreed most consistently and without apparent interference from other peaks. Thus, these two values were averaged. The 114 and 11$\bar{4}$ peaks also are diagnostic of the $2M_1$ polytype of illite, but, in the XRD tracing shown in figure 2, the 11$\bar{4}$ peak has interference from the fourth-order chlorite peak and perhaps a weak anatase peak, and the 114 peak shows interference by a feldspar peak. For the $1M$ polytype, the 11$\bar{2}$, 112, and 023 peaks are diagnostic. Illite is a relatively weak diffractor of x-rays, and these diagnostic peaks have low intensities relative to the most intense illite peaks.

Figure 2 XRD tracing (CuKα) of a random powder of the <2-μm fraction of the Browning Sandstone. Numbers are Miller indices of peaks of the $2M_1$ and $1M$ polytypes of illite with diagnostic peaks crosshatched for the $2M_1$. The {114} peaks normally are diagnostic, but in this case are interfered with by chlorite and feldspar peaks. The small arrows point to the position on the tracings for diagnostic peaks for the $1M$ polytype. Chl-4 is the fourth order of the basal series of chlorite; Il-3 is the third order of the basal series of illite; Kao-2 is the second order of the basal series of kaolinite; and Qtz is quartz. The f marks the small peaks of feldspars.

RESULTS

Approximate modal analyses of the bulk Browning Sandstone (table 1) were based on XRD using the RIR method described by Hughes et al. (1994). Sample numbers are the petrographic numbers of the Clay Lab at the Illinois State Geological Survey. Sample 3700A is the top, 3700B is the middle, and 3700C is at the water level of the type section. Where the Browning Sandstone is massive, the quartz content is greater; where it is flaggy, the illite content is greater. The illite plus muscovite (IL/Mus) category of the Browning Sandstone in table 1 represents mica, illite, and I/S combined.

Results from probing feldspar grains (72 analyses of 59 grains) are given in table 2 and plotted in figure 3. For the Na:K:Ca ratio in feldspar grains from the Browning Sandstone, 25 grains have ≥90% Na, and 34 have ≥90% K, a bimodal distribution. The average Na:K:Ca ratio for the 72 analyses of 59 feldspar grains is (45.0 ± 45.1):(53.7 ± 45.9):(1.3 ± 2.5). Distribution is, perhaps, better shown in figure 4.

Table 1 Modal analyses of three representative samples of the Browning Sandstone from the type section.

Sample[1]	Qtz-1	IL/Mus 002	Kao 001	Chl 003	Kf 27.5[2]	Pf 28[2]	Sum
3700A	57	18	11	6	1	7	100
3700B	65	15	9	4	1	6	100
3700C	51	25	11	6	1	7	101[3]

[1] Sample numbers are the petrographic numbers of the Clay Laboratory at the Illinois State Geological Survey. Sample 3700A is the top, 3700B is the middle, and 3700C is at the water level of the type section.
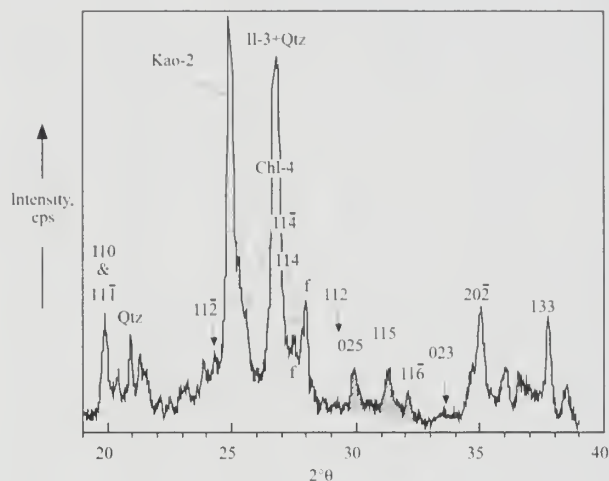[2] 2θ positions (CuKα) used for these two minerals.
[3] From a rounding error.

Table 2 Na:K:Ca ratios of silt-size feldspar grains from the Browning Sandstone.

Grain no.	Na	K	Ca	Grain no.	Na	K	Ca
1	89.4	0.0	10.6	28	0.0	98.5	1.5
2	21.1	78.9	0.0	29	84.9	13.3	1.8
2A	26.3	73.7	0.0	30	98.6	0.0	1.4
3	97.5	1.2	1.3	31	97.4	0.9	1.7
4	9.4	89.1	1.5	32	94.3	5.7	0.0
4A	19.6	80.4	0.0	33	0.0	100.0	0.0
5	100.0	0.0	0.0	33A	0.0	100.0	0.0
6	97.4	1.3	1.3	34	0.0	100.0	0.0
7	100.0	0.0	0.0	35	7.8	92.2	0.0
8	0.0	100.0	0.0	36	96.3	1.9	1.8
9	0.0	100.0	0.0	37	100.0	0.0	0.0
10	3.2	96.8	0.0	38	65.7	30.2	4.1
11	0.0	97.8	2.2	39	5.4	92.8	1.8
11A	16.7	81.4	1.8	40	0.0	100.0	0.0
12	100.0	0.0	0.0	41	72.7	27.3	0.0
13	4.5	95.5	0.0	41A	0.0	98.1	1.9
13A	0.0	100.0	0.0	42	3.7	96.3	0.0
14	0.0	98.3	1.7	43	100.0	0.0	0.0
15	4.5	95.5	0.0	44	100.0	0.0	0.0
15A	11.5	88.5	0.0	45	68.7	31.3	0.0
16	90.8	1.1	8.1	45A	0.0	100.0	0.0
17	97.8	1.2	1.0	46	100.0	0.0	0.0
18	0.0	100.0	0.0	48	0.0	100.0	0.0
18A	0.0	97.6	2.4	49	92.4	6.1	1.4
19	100.0	0.0	0.0	50	98.6	0.0	1.4
20	4.2	95.8	0.0	51	0.0	100.0	0.0
21	9.6	90.4	0.0	52	0.0	98.5	1.5
22	5.4	94.6	0.0	53	84.3	6.6	9.1
22A	5.4	92.1	2.4	53A	87.7	1.4	10.9
23	0.0	100.0	0.0	53B	91.5	1.2	7.3
24	80.4	14.5	5.1	54	100.0	0.0	0.0
25	3.5	96.5	0.0	55	100.0	0.0	0.0
25A	5.4	94.6	0.0	56	95.0	2.4	2.6
26	0.0	100.0	0.0	57	96.0	0.0	4.0
26A	4.8	93.8	1.4	58	97.0	1.2	1.7
27	0.0	100.0	0.0	59	91.3	8.7	0.0
				Avg.	45.0	53.7	1.3
				SD	45.1	45.9	2.5

For mica, 60 grains yielded 81 analyses (table 3). The average structural formula for a half-unit[1] cell for the 80 analyses from the Browning Sandstone is

$$(K_{0.825}Na_{0.055}Ca_{0.010})(Al_{1.71}Mg_{0.175}Fe_{0.185}Ti_{0.035})(Si_{3.115}Al_{0.885})O_{10}(OH)_2.$$

The interlayer cations of the average mica of the Browning Sandstone neutralize a layer charge of 0.90. The average cation proportions and first standard deviations of the interlayer cations for a half-unit cell in the Browning Sandstone are 0.825 ± 0.20 K, 0.055 ± 0.105 Na, and 0.01 ± 0.015 Ca (tables 3 and 4), or, based on a whole unit cell as in table 3, 1.65 ± 0.40K, 0.11 ± 0.21Na, and 0.02 ± 0.03 Ca.

Satisfactory reproducibility was obtained from triplicate analyses of laboratory standards before starting an analytical session. Precision also was measured by 10-fold replication of analyses on a single mica grain (table 4) from the Browning Sandstone, which showed $6.27 \pm 0.14\%$ Si atoms per formula unit.

An XRD tracing of an oriented aggregate of clay minerals from the Browning Sandstone is shown in figure 5. Also shown in figure 5 are XRD tracings from an oriented aggregate of the <2-μm fraction of a shale from the Ordovician Maquoketa Group, a unit that has been particularly well characterized (Grathoff and Moore 1996), and from

[1]Chemists and mineralogists use half-unit cells in chemical formulas to describe minerals other than clay minerals, a variation from the conventional method, which uses whole-unit cells.

Table 3 Proportions of cations in silt-size mica flakes from the Browning Sandstone based on 22 oxygens (whole unit cell).

Grain no.	IV Si	IV Al	Charge	VI Al	VI Mg	VI Fe	VI Ti	Oct.[1] Cations	Charge	Total layer charge	Interlayer cation K	Interlayer cation Na	Interlayer cation Ca	IC + charge	Mol% Na[2]	Total weight
1	6.37	1.63	1.63	2.69	0.66	0.45	0.33	4.13	0.404	2.04	2.04	0.00	0.00	2.04	0.00	97.23
2	6.38	1.62	1.62	4.32	0.12	0.00	0.00	4.44	-1.210	0.41	0.41	0.00	0.00	0.41	0.00	83.91
2A	6.16	1.84	1.84	3.67	0.25	0.08	0.10	4.10	-0.060	1.78	1.56	0.22	0.00	1.78	12.40	94.24
3	6.13	1.87	1.87	3.53	0.32	0.08	0.09	4.02	0.253	2.12	1.85	0.18	0.05	2.12	8.50	95.48
3A	6.14	1.87	1.87	3.63	0.31	0.06	0.07	4.07	0.076	1.94	1.84	0.09	0.00	1.94	4.90	94.77
4	6.20	1.80	1.80	3.75	0.22	0.10	0.04	4.12	-0.060	1.73	1.73	0.00	0.00	1.73	0.00	92.54
5	6.12	1.89	1.89	3.43	0.31	0.36	0.08	4.17	0.080	1.97	1.87	0.09	0.00	1.96	4.60	94.02
5A	6.51	1.49	1.49	3.33	0.27	0.41	0.00	4.01	0.654	2.14	1.67	0.16	0.16	2.14	8.00	73.18
6	6.19	1.81	1.81	3.50	0.31	0.40	0.06	4.26	-0.130	1.69	1.69	0.00	0.00	1.69	0.00	81.31
8	6.10	1.90	1.90	3.61	0.43	0.07	0.04	4.15	0.005	1.90	1.52	0.38	0.00	1.90	20.00	100.61
8A	6.34	1.66	1.66	3.79	0.32	0.00	0.00	4.10	0.011	1.67	1.67	0.00	0.00	1.67	0.00	95.03
9	6.15	1.85	1.85	3.48	0.27	0.14	0.14	4.03	0.182	2.03	1.91	0.00	0.06	2.03	0.00	96.23
9A	6.24	1.77	1.77	3.65	0.20	0.14	0.06	4.05	0.141	1.91	1.91	0.00	0.00	1.91	0.00	93.48
11	6.00	2.00	2.00	3.53	0.30	0.20	0.10	4.14	-0.010	1.98	1.80	0.19	0.00	1.99	9.40	96.67
11A	6.14	1.86	1.86	3.72	0.16	0.22	0.04	4.13	-0.040	1.81	1.81	0.00	0.00	1.81	0.00	96.03
12	6.18	1.82	1.82	3.08	0.50	0.56	0.08	4.23	0.281	2.10	1.74	0.17	0.10	2.10	8.60	97.37
13	6.26	1.74	1.74	3.52	0.21	0.47	0.00	4.19	0.096	1.84	1.84	0.00	0.00	1.84	0.00	91.58
13A	6.22	1.79	1.79	3.45	0.27	0.48	0.00	4.20	0.140	1.93	1.81	0.00	0.06	1.93	0.00	94.95
13B	6.14	1.86	1.86	3.61	0.15	0.42	0.00	4.17	0.046	1.90	1.90	0.00	0.00	1.90	0.00	94.01
14	6.28	1.72	1.72	3.78	0.29	0.00	0.00	4.08	0.066	1.79	1.24	0.36	0.09	1.79	21.40	80.60
14A	6.20	1.80	1.80	3.79	0.36	0.00	0.00	4.15	-0.090	1.71	1.22	0.39	0.05	1.71	23.70	89.81
15	6.17	1.83	1.83	3.95	0.11	0.24	0.11	4.41	-0.990	0.84	0.35	0.48	0.00	0.84	57.60	86.87
15A	6.16	1.85	1.85	3.94	0.13	0.14	0.00	4.21	-0.360	1.48	0.29	1.20	0.00	1.48	80.70	95.81
16	6.25	1.75	1.75	2.99	0.45	0.60	0.15	4.18	0.356	2.11	1.85	0.15	0.06	2.11	7.10	91.40
16A	6.46	1.54	1.54	3.40	0.25	0.43	0.10	4.18	0.046	1.59	1.58	0.00	0.00	1.58	0.00	84.10
17	6.67	1.33	1.33	2.90	0.73	0.63	0.00	4.26	0.574	1.90	1.91	0.00	0.00	1.91	0.00	93.41
19	6.29	1.71	1.71	3.31	0.39	0.44	0.08	4.22	0.092	1.80	1.81	0.00	0.00	1.81	0.00	95.56
19A	6.24	1.77	1.77	3.25	0.37	0.44	0.13	4.19	0.108	1.87	1.87	0.00	0.00	1.87	0.00	95.35
20	6.29	1.71	1.71	3.83	0.27	0.00	0.08	4.17	-0.330	1.39	1.39	0.00	0.00	1.39	0.00	87.23
20A	6.12	1.88	1.88	3.52	0.41	0.08	0.15	4.15	-0.130	1.75	1.61	0.00	0.07	1.74	0.00	94.87
21	6.20	1.80	1.80	4.01	0.11	0.15	0.00	4.27	-0.540	1.26	0.16	1.10	0.00	1.26	87.50	91.19
21A	6.19	1.81	1.81	4.02	0.10	0.17	0.00	4.29	-0.600	1.21	0.34	0.86	0.00	1.20	71.70	88.20
22	6.29	1.71	1.71	2.95	0.59	0.56	0.14	4.23	0.311	2.02	2.02	0.00	0.00	2.02	0.00	96.63
22A	6.30	1.70	1.70	2.87	0.53	0.62	0.21	4.22	0.272	1.97	1.97	0.00	0.00	1.97	0.00	96.88
23	6.16	1.84	1.84	3.30	0.32	0.59	0.09	4.30	-0.080	1.76	1.76	0.00	0.00	1.76	0.00	94.57
23A	6.10	1.90	1.90	3.31	0.30	0.57	0.10	4.29	-0.090	1.81	1.81	0.00	0.00	1.81	0.00	92.47
24	6.05	1.95	1.95	3.62	0.26	0.11	0.10	4.09	0.005	1.96	1.71	0.24	0.00	1.95	12.20	97.74
24A	6.20	1.80	1.80	3.79	0.16	0.10	0.06	4.11	-0.140	1.67	1.66	0.00	0.00	1.66	0.00	94.74
25	6.28	1.72	1.72	3.73	0.19	0.11	0.04	4.06	0.068	1.79	1.79	0.00	0.00	1.79	0.00	94.36
26	6.08	1.92	1.92	3.34	0.36	0.41	0.12	4.22	-0.020	1.90	1.74	0.16	0.00	1.89	8.20	96.16
28	6.29	1.71	1.71	3.47	0.30	0.44	0.00	4.20	0.127	1.84	1.84	0.00	0.00	1.84	0.00	95.29
28A	6.31	1.69	1.69	3.61	0.27	0.34	0.00	4.21	-0.040	1.65	1.54	0.00	0.06	1.65	0.00	87.00
29	6.17	1.83	1.83	3.65	0.18	0.30	0.00	4.13	0.100	1.93	1.64	0.21	0.04	1.93	11.10	95.12
29A	6.12	1.88	1.88	3.62	0.21	0.27	0.06	4.15	-0.020	1.86	1.65	0.21	0.00	1.86	11.20	94.06
30	6.23	1.77	1.77	3.43	0.26	0.45	0.06	4.20	0.054	1.82	1.73	0.00	0.05	1.82	0.00	92.69
30A	6.18	1.82	1.82	3.36	0.35	0.39	0.07	4.16	0.180	2.00	1.70	0.22	0.04	2.00	11.30	95.89
33	6.57	1.43	1.43	3.43	0.35	0.45	0.00	4.23	0.114	1.54	1.54	0.00	0.00	1.54	0.00	93.74
33A	6.41	1.60	1.60	3.47	0.43	0.44	0.03	4.37	-0.280	1.32	1.32	0.00	0.00	1.32	0.00	94.95
34	6.23	1.78	1.78	3.32	0.35	0.31	0.13	4.10	0.227	2.00	1.87	0.13	0.00	2.00	6.60	96.64
34A	6.30	1.70	1.70	3.32	0.31	0.31	0.10	4.04	0.410	2.11	1.83	0.20	0.04	2.11	9.40	93.74
35	6.34	1.67	1.67	3.01	0.53	0.74	0.05	4.32	0.253	1.92	1.92	0.00	0.00	1.92	0.00	96.54
35A	6.35	1.65	1.65	3.10	0.40	0.62	0.06	4.17	0.432	2.08	2.08	0.00	0.00	2.08	0.00	93.02
35B	6.24	1.76	1.76	3.48	0.24	0.42	0.04	4.18	0.092	1.86	1.85	0.00	0.00	1.85	0.00	94.89

Table 3 (continued) Proportions of cations in silt-size mica flakes from the Browning Sandstone based on 22 oxygens (whole unit cell).

Grain no.	IV			VI				Oct.[1]		Total layer	Interlayer cation			IC +	Mol%	Total
	Si	Al	Charge	Al	Mg	Fe	Ti	Cations	Charge	charge	K	Na	Ca	charge	Na[2]	weight
36	5.08	2.92	2.92	0.78	1.77	3.54	0.36	6.45	-2.380	0.54	0.37	0.00	0.09	0.55	0.00	80.34
37	6.26	1.75	1.75	3.11	0.43	0.55	0.11	4.20	0.271	2.02	2.01	0.00	0.00	2.01	0.00	93.09
38	6.17	1.83	1.83	3.84	0.24	0.12	0.00	4.20	-0.240	1.59	1.59	0.00	0.00	1.59	0.00	93.35
39	6.21	1.79	1.79	3.13	0.48	0.62	0.09	4.32	0.047	1.84	1.84	0.00	0.00	1.84	0.00	96.63
39A	6.33	1.67	1.67	3.27	0.34	0.54	0.06	4.21	0.193	1.87	1.87	0.00	0.00	1.87	0.00	93.59
41	6.54	1.46	1.46	3.30	0.55	0.20	0.03	4.09	0.454	1.91	1.79	0.13	0.00	1.91	6.60	95.73
41A	6.48	1.52	1.52	3.53	0.44	0.15	0.00	4.11	0.251	1.77	1.77	0.00	0.00	1.77	0.00	93.39
42	6.25	1.75	1.75	3.25	0.43	0.48	0.10	4.26	0.028	1.78	1.66	0.11	0.00	1.77	6.20	95.10
42A	6.28	1.72	1.72	3.29	0.28	0.58	0.05	4.20	0.203	1.92	1.93	0.00	0.00	1.93	0.00	93.98
43	6.40	1.60	1.60	3.51	0.20	0.41	0.00	4.12	0.250	1.85	1.84	0.00	0.00	1.84	0.00	91.79
44	6.74	1.27	1.27	3.04	0.77	0.50	0.00	4.31	0.333	1.60	1.58	0.00	0.05	1.68	0.00	95.07
46	6.18	1.83	1.83	3.27	0.39	0.52	0.09	4.27	0.024	1.85	1.85	0.00	0.00	1.85	0.00	93.67
46A	6.22	1.78	1.78	3.40	0.25	0.44	0.11	4.20	-0.010	1.77	1.77	0.00	0.00	1.77	0.00	91.59
47	6.13	1.87	1.87	3.76	0.24	0.08	0.04	4.13	-0.110	1.76	1.53	0.23	0.00	1.76	12.90	87.20
47A	6.13	1.87	1.87	3.74	0.19	0.10	0.07	4.10	-0.090	1.77	1.45	0.32	0.00	1.77	17.90	95.20
49	6.16	1.84	1.84	3.53	0.29	0.09	0.15	4.06	0.041	1.88	1.78	0.10	0.00	1.88	5.50	95.94
49A	6.18	1.83	1.83	3.35	0.34	0.38	0.10	4.15	0.155	1.98	1.76	0.21	0.00	1.98	10.80	92.76
51	6.23	1.77	1.77	3.42	0.26	0.46	0.05	4.19	0.107	1.88	1.88	0.00	0.00	1.88	0.00	94.20
51A	6.14	1.86	1.86	3.29	0.25	0.52	0.08	4.14	0.279	2.14	1.94	0.11	0.04	2.13	5.10	97.44
52	6.34	1.66	1.66	3.17	0.62	0.56	0.00	4.35	0.131	1.79	1.70	0.00	0.05	1.79	0.00	90.63
52A	6.44	1.56	1.56	3.21	0.32	0.62	0.04	4.19	0.323	1.88	1.88	0.00	0.00	1.88	0.00	84.21
54	6.25	1.75	1.75	3.94	0.14	0.00	0.03	4.11	-0.240	1.52	1.32	0.19	0.00	1.52	12.60	89.57
54A	6.13	1.87	1.87	3.85	0.18	0.10	0.06	4.20	-0.380	1.49	1.09	0.27	0.06	1.48	19.20	95.29
59	6.08	1.92	1.92	3.62	0.21	0.14	0.11	4.07	0.039	1.96	1.70	0.15	0.05	1.96	7.80	95.85
59A	6.10	1.90	1.90	3.61	0.27	0.11	0.09	4.08	0.052	1.96	1.74	0.11	0.05	1.96	5.50	91.58
60	6.27	1.73	1.73	3.48	0.32	0.34	0.05	4.18	0.069	1.80	1.67	0.13	0.00	1.80	7.10	94.94
60A	6.25	1.76	1.76	3.63	0.23	0.33	0.00	4.19	-0.020	1.74	1.74	0.00	0.00	1.74	0.00	93.04
Avg.	6.23	1.77	1.77	3.42	0.35	0.37	0.07	4.21	0.030	1.80	1.65	0.11	0.02	1.80	6.10	92.78
SD	0.18	0.18	0.18	0.41	0.21	0.39	0.07	0.25	0.380	0.29	0.40	0.21	0.03	0.29	32.70	4.98

[1]Octahedral.
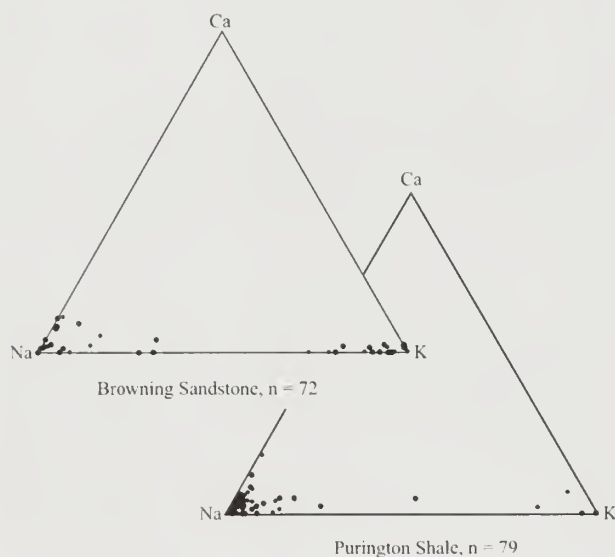[2]Molar percentage of cations in the interlayer space.

Figure 3 Ternary plots of the modal composition of the 3.5- to 4-ϕ feldspar grains (0.09 to 0.0625 mm) of the Browning Sandstone and the Purington Shale.

the Purington Shale (Moore 2000), which is approximately the same age as the Browning Sandstone (fig. 1). These characterizations allow a comparison of the clay mineral contents of these Pennsylvanian units with a representative lower Paleozoic shale, all from the Illinois Basin. They are strikingly similar. Using XRD tracings of random powders of size fractions and based on the methods of Grathoff and Moore (1996), the Browning Sandstone has 66% $2M_1$ and 34% $1M$ and $1M_d$ in the <1-µm fraction and 70% $2M_1$, and 30% $1M$ and $1M_d$ in the <2-µm fraction (fig. 2). Using a second method, as described by Gharrabi et al. (1998), peak areas from decomposition of an XRD tracing of an oriented aggregate of the <1-µm fraction of the Browning Sandstone yielded between 55 to 61% $2M_1$ and 39 and 45% $1M$ and $1M_d$.

DISCUSSION

The feldspars, micas, and clay minerals of the Browning Sandstone show evidence of subtle diagenetic changes. These changes are most apparent when these minerals are compared with the nearby Purington Shale (Moore 2000).

Feldspars

The compositional distribution of feldspars in the Browning Sandstone (figs. 3 and 4) differs from that of modern detrital suites of feldspars in that the Browning Sandstone lacks any Ca-rich feldspars and few alkali feldspars of intermediate composition, whereas the common pattern of modern detrital feldspar assemblages is a full range of compositions (fig. 6) (Charles and Blatt 1978, Trevena and Nash 1979, Milliken et al. 1989). The primary source area for the detritus that formed the Mississippian and Pennsylvanian clastic rocks of the Upper Mississippi Valley was identified generally by Potter and Pryor (1961) as the Canadian Shield and the tectonic borderlands of the northern Appalachian Mountains. Throughout this time of deposition, the general slope of the craton in the region of the Illinois Basin and adjacent areas had a relatively low gradient tending

generally to the south. Mapping of the meandering, generally south to southwest-oriented channels that cut into the coals in the Illinois Basin emphasize this point (Treworgy and Jacobson 1985). According to maps of Potter and Siever (1956), Siever and Potter (1956), and Laury (1968), showing the direction of drainages into the northern and northwestern parts of the Illinois Basin, the Pennsylvanian clastics on the Western Shelf, including the Browning Sandstone, were derived from older sedimentary rocks, the Transcontinental Arch, and quartzofeldspathic terrains in the Lake Superior and Lake Huron regions of the Canadian Shield. Low gradients tend to deliver feldspar grains that are only moderately abraded, whereas in streams of steeper gradients, feldspars are commonly lost to abrasion (Potter and Glass 1958); therefore, Pennsylvanian clastics delivered by these gentle gradients should have included moderately abraded feldspars. When deposited, these sediments should have a full compositional range of feldspars.

The areas identified as the primary sources for Paleozoic clastics were crossed by continental ice sheets that spread over the Midwest. The Quaternary glacial deposits of Illinois are thought to have incorporated material from the Canadian Shield that is similar to sources of sediments for the Browning Sandstone. In Illinois, Frye et al. (1962) reported that glacial outwash and loess contain K-feldspar and Na-Ca-feldspar in the very fine and fine sand fractions. Although the data of Frye et al. (1962) imply a range of compositions, their feldspars need to be analyzed with modern instruments to discern the actual spread. Glacial erratics scattered over the landscape, which range from gab-
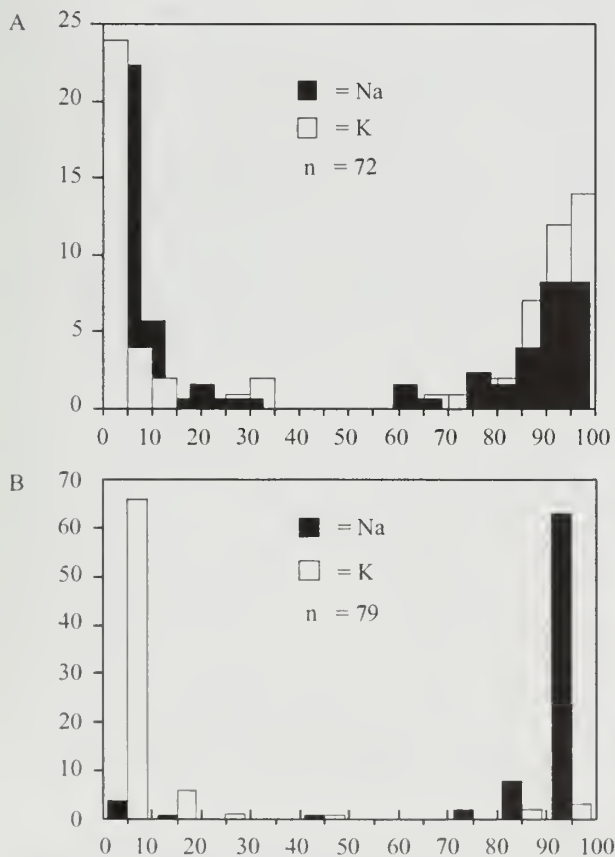

Figure 4 Comparison of the distribution of the Na and K occupancies in silt-size feldspar grains from the Browning Sandstone (A) and the Purington Shale (B). Ca occurs so seldom (table 2) that it is omitted, but it is considered in the calculations.
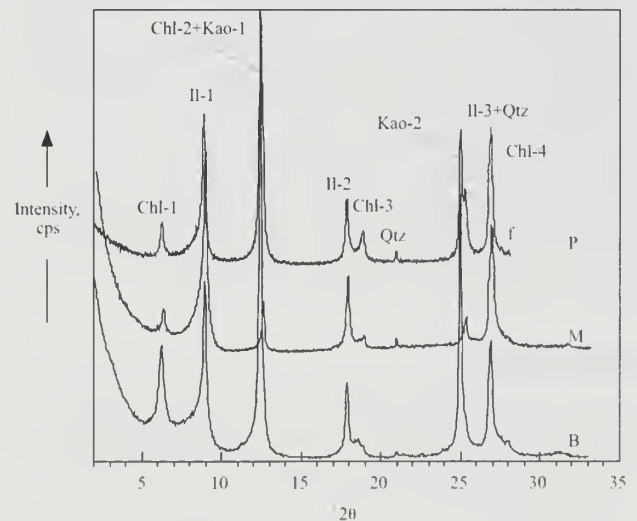

Figure 5 XRD tracings (CuKα) of air-dried, oriented aggregates of clay minerals from the <2-μm fraction of the Purington Shale (P), the Maquoketa Group (M), and the Browning Sandstone (B). Chl-1 is the first order of the basal series of chlorite, Chl-2 second order, followed by Chl-3 and Chl-4; Il is illite; Kao is kaolinite; and Qtz is quartz. The f marks the small peak of a feldspar.
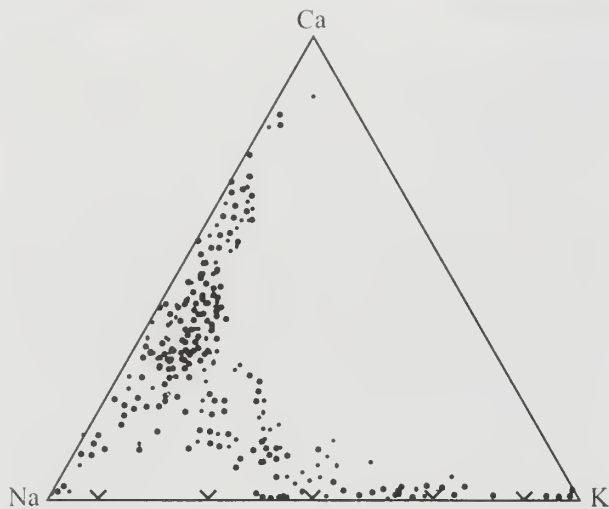
Figure 6 Ternary plots showing the spread of composition of feldspar grains from five "least-altered" Oligocene Frio Formation samples; n is 264 (redrawn after Milliken et al. 1989).

broic to granitic support the supposition that the feldspars of Frye et al. (1962) have a full range of composition. In addition, Milliken (1988) plotted 47 feldspar compositions from the >0.062-mm fractions of current Mississippi River sands and 108 from Pleistocene Gulf of Mexico sedimentary rocks buried at ≤450 m. Further, Milliken et al. (1989) presented 264 analyses from their choice of the least-altered samples of the Oligocene Frio Formation (fig. 6) and 103 feldspar analyses from modern Rio Grande River sands. All show a full range of compositions (for example, compare the distribution of feldspar compositions shown in fig. 6 with those of fig. 3). These several lines of evidence indicate that the currently observable distribution of feldspar compositions in the Browning Sandstone is quite different from its original detrital composition and from modern assemblages and that the feldspars eroded from the ancient source areas for Pennsylvanian clastics must have been similar to the modern assemblages before burial and diagenesis. These inferences strongly suggest diagenetic alteration of the feldspars in the Browning Sandstone.

Mica and Illite

The Browning Sandstone contains mica, illite, and illite-rich I/S. Persuasive arguments have been made that illite and muscovite each have unique chemical and structural characteristics (Meunier and Velde 1989, Środoń et al. 1992, Gharrabi et al. 1998). The term "illite" in this report indicates the clay mineral that gives a relatively broad peak representing a repeat distance along the crystallographic Z direction of about 10Å (8.8°2θ in figs. 5 and 7) and may include amounts of expandable layers up to ~10% interlayered with illite. "Mica," as used in this report, has a narrower peak than illite and has a peak position 0.1 to 0.2Å

smaller than that of illite. Because illite crystallites have fewer layers than mica along the crystallographic section, the 001 illite peak is slightly shifted up the steep background slope of the Lorenz-polarization background at this position (Moore and Reynolds 1997). The illite peak also is broader than that of mica because of its smaller coherent diffracting domain. With care, a sharper peak for the mica can be resolved from the broader peak at the position of their 001 peaks (Lanson and Champion 1991). Figure 7 shows the results of the decomposition of these peaks from which background has been subtracted. Here "mica" is called well-crystallized illite (WCI) and "regular" illite is called poorly crystallized illite (PCI), as these terms were used by Gharrabi et al. (1998). An illite-rich I/S also is resolved by peak decomposition. Part of the asymmetry of broad peaks at about 8.85°2θ (CuKα) or less is due to the steep slope of the Lorenz-polarization background (Moore and Reynolds 1997). However, to emphasize that additional asymmetry is indeed due to peaks on the low-angle side of the peak of a WCI, it should be noted that the peak for chlorite in figure 7, sitting on the same steep slope, is symmetrical, or, if the chlorite peak were to be judged asymmetrical, the asymmetry is on the opposite side of the complex peak at 8.85°2θ.

A comparison of the composition of the 0.090- to 0.063-mm mica grains from the Browning Sandstone with that from selected analyses of muscovites from Deer et al. (1962, p. 16–18) and of illites with small amounts of expandable material from Newman and Brown (1987, p. 72–73) shows that micas from the Browning Sandstone have an amount of interlayer cations that is part way between mica and illite. Curiously, electron microprobe results show compositions from muscovite to potassium-rich paragonite, ranging from Mu_{100} to $Mu_{13}Pg_{87}$ (e.g., see grain 21, table 3). This appar-
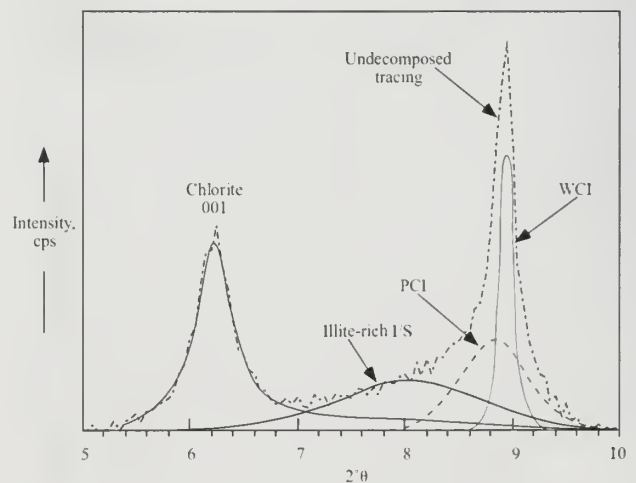

Figure 7 A decomposition of the peak near 8.8°2θ (CuKα) of the Browning Sandstone from its type section. This tracing is from a random powder of the same sample as that used for the oriented aggregate tracing B in figure 5. I/S is illite/smectite; PCI and WCI are poorly and well-crystallized illite, respectively.

Grain no.	IV			VI				Oct.[1]		Total layer	Interlayer cation			IC +	Mol%	Total
	Si	Al	Charge	Al	Mg	Fe	Ti	Cations	Charge	charge	K	Na	Ca	charge	Na[2]	weight
1	6.37	1.63	1.63	2.69	0.66	0.45	0.33	4.13	0.404	2.04	2.04	0.00	0.00	2.04	0.00	97.23
1A	6.12	1.88	1.88	3.34	0.36	0.53	0.04	4.27	0.043	1.92	1.92	0.00	0.00	1.92	0.00	85.46
1B	6.17	1.83	1.83	3.36	0.36	0.50	0.05	4.28	-0.010	1.82	1.82	0.00	0.00	1.82	0.00	94.00
1C	6.17	1.84	1.84	3.24	0.38	0.59	0.08	4.28	0.053	1.89	1.89	0.00	0.00	1.89	0.00	94.83
1D	6.25	1.76	1.76	3.30	0.45	0.24	0.09	4.09	0.344	2.10	1.93	0.17	0.00	2.10	8.00	98.34
1E	6.21	1.79	1.79	3.28	0.36	0.57	0.07	4.28	0.018	1.81	1.81	0.00	0.00	1.81	0.00	94.13
1F	6.13	1.87	1.87	3.20	0.37	0.54	0.10	4.20	0.204	2.07	1.86	0.00	0.10	2.07	0.00	72.26
1G	6.55	1.45	1.45	2.79	0.63	0.37	0.29	4.08	0.481	1.93	1.93	0.00	0.00	1.93	0.00	94.30
1H	6.36	1.64	1.64	2.99	0.71	0.35	0.17	4.23	0.213	1.86	1.85	0.00	0.00	1.85	0.00	96.41
1I	6.33	1.67	1.67	3.40	0.38	0.23	0.04	4.05	0.427	2.10	1.99	0.00	0.06	2.10	0.00	95.64
Avg.	6.27	1.74	1.74	3.16	0.47	0.44	0.13	4.19	0.218	1.95	1.90	0.02	0.02	1.95	0.80	92.26
SD	0.14	0.14	0.14	0.25	0.14	0.13	0.10	0.09	0.187	0.11	0.07	0.05	0.04	0.11	2.53	7.84

[1]Octahedral.
[2]Molar percentage of cations in the interlayer space.

ently continuous range of values may have resulted from the beam spot of the microprobe being too large. Shau et al. (1991) and Guidotti and Sassi (1998) emphasized that on the scale of high resolution transmission electron microscopy (HRTEM), muscovite and paragonite tend to be segregated. The Na content of analysis 1D (table 4), which is the only one of the 10 analyses of the same mica flake to record Na, supports the suspicion that the beam spot was too large and that segregation occurs within the mica flake of K- and Na-rich crystals. Sodium-potassium micas are generally associated with prehnite-pumpellyite to amphibolite or eclogite facies of metabasic rocks (Shau et al. 1991 and references therein). At commonly accepted temperature ranges for diagenesis, solid solution series between these two end members should be quite limited (Guidotti and Sassi 1998), which suggests that the micas are detrital and are more resistant to diagenetic change than are the feldspars. Conversely, the average interlayer charge of micas is less than the full complement of 1.00 per half formula unit (0.90, table 4), which suggests either that these micas were delivered to the depositional environment in a weathered state and did not pick up additional interlayer cations from their marine environment or that they did become "reconstituted" by exposure to the marine environment and since then have been diagenetically altered. In basins to which weathered micas have been delivered, it should at least be considered that in the process of reconstitution the micas would be expected to absorb potassium. If this is the case, later diagenesis may be responsible for removing some of the potassium from the micas of the Browning Sandstone.

Clay Mineralogy

Even though the effects of burial on the Browning Sandstone cannot be tracked because the unit has not been buried deeply enough and does not extend southeastward from the western shelf into the deep part of the Illinois Basin, the clay mineralogy supports the conclusion that there has been significant diagenetic alteration of the originally deposited sedimentary material. There is diagenetic and detrital illite in the Browning Sandstone. The diagenetic portion has ≤10% smectite layers. These are the $1M$ and $1M_d$ polytypes and form the PCI and illite-rich I S peaks in figure 7.

Grathoff and Moore (1996), reporting on shales of the Ordovician Maquoketa Group, found illitic clay minerals dominated by PCI and illite-rich I S to be very similar to those of the Browning Sandstone (fig. 5). Gharrabi and Velde (1995) measured changes in I S with depth through shales of the Paleozoic column in one of the deepest drill holes in the Illinois Basin (~2800 m) and in samples of shales of the New Albany Group from drill holes throughout the basin. Although Gharrabi and Velde found a slight decrease in the amount of smectite in the I S in the deepest drill hole, all of the mineralogy they reported is essentially the same—WCI, PCI, and illite-rich I S. Moore (2000) found the clay minerals of the Purington Shale, a unit in the same Desmoinesian cyclothem as the Browning Sandstone (fig. 1), to be almost identical. Therefore, the I S in the Browning Sandstone is generally the same as that of other Paleozoic units in the Illinois Basin.

As another example of low-temperature, time-dependent diagenesis, but outside the Illinois Basin, Kirsimäe et al. (1999) and Kirsimäe and Jorgensen (2000) reported significant diagenetic changes in Early Cambrian unconsolidated clays and silty clays, deposited under normal marine conditions on the Eastern European platform. Those authors identified diagenetically formed illite with ≤5% expandable layers in the unit they investigated and concluded that maximum burial depth did not exceed ~800 to 1000 m and that the rocks were subjected to temperatures of no more than about 35°C.

This accumulation of findings supports the conclusion that a significant portion of the 2:1 clay minerals originally delivered to the environment of deposition of the Browning Sandstone, all other Paleozoic clastics in the Illinois Basin, and probably most cratonic Paleozoic clastics must have been composed of significant amounts of smectite-rich I/S, which has been, and continues to be, diagenetically transformed to an I/S that has ≥90% illite layers.

One way in which the illite of the Browning Sandstone is different from that of the Purington Shale is that, within the margin of error, polytype amounts are the same in both size fractions, whereas in the Purington Shale, the amount of $2M_1$ polytype decreases with decreasing particle size. The ways in which polytypes of illite and illite-rich I/S can be used to discriminate between detrital and diagenetic illites and as indicators of diagenetic history have been discussed by Grathoff and Moore (1996), Grathoff et al. (1998), and Pevear (1992, 1999). These scientists have shown that two significant changes occur with a decrease in particle size of illite and I/S. The K/Ar age of the size fraction decreases to well below the stratigraphic age of the unit being considered, and the proportion of $1M$ and $1M_d$ polytypes increases relative to the $2M_1$ polytype. On this basis, these researchers concluded that (1) the $2M_1$ polytype of illite is detrital even if it has been partly restructured by incorporating additional K^+, and (2) the $1M$ and $1M_d$ polytypes are diagenetic.

What seems clear is that the Browning Sandstone and the Purington Shale apparently took somewhat different diagenetic paths, but both are examples of low-temperature, time-dependent diagenesis. The feldspars, the micas, and the clay minerals are slightly, but significantly, different. The composition of the feldspars of the Browning Sandstone is bimodally distributed with approximately equal amounts of Na-rich and K-rich feldspars and a complete absence of Ca-rich feldspars, whereas the bulk of the Purington feldspars are crowded into the albite corner of the diagram (fig. 3). The compositions of the micas of the Browning Sandstone range from muscovitic to paragonitic (table 3), whereas those of the Purington Shale show only minor amounts of Na. Approximately 60% of the clay minerals of both units consist of a combination of PC1, WC1, and illite-rich I/S. Kaolinite and chlorite make up about 40% of the clay minerals, but the diagenetic information they hold is not yet clearly understood. Kaolinite is a common product of the weathering of feldspars, but that is an improbable explanation for the kaolinite in these two units. Although both contain detrital and diagenetic illite, the pattern of change in the proportions of polytypes is different with changes in particle size, most probably related to physical differences between sandstones and shales (Pevear 1999). The most likely basis for this difference is permeability; that is, the system was more open for the Browning Sandstone than for the Purington Shale.

One other observation from the Browning Sandstone is that its chlorite seems to have been vermicularized. As shown in figure 5, the chlorite in the Browning Sandstone has the most intense first-order chlorite peak of the three tracings, and yet its third-order peak (near 18.8°2θ) is broadened, less intense than expected, and shifted in the low-angle direction from the position of a "normal" chlorite. The partial alteration to vermiculite, indicated by this peak shape and position, is more likely to be an effect of weathering at the outcrop than of diagenesis. The difference may be that, when collected, samples of the chlorite-containing Purington Shale and of the Maquoketa Group were less weathered than those of the Browning Sandstone, or perhaps the lower permeability of the two shales relative to the sandstone allowed less fluid to pass through them, or both.

SUMMARY AND CONCLUSIONS

The feldspars, micas, and clay minerals of the Browning Sandstone show that it has undergone extensive low-temperature, time-dependent diagenesis. Diagenesis of this Pennsylvanian sandstone differs from that which modified Cenozoic and Mesozoic sediments of the U.S. Gulf Coast in similar depositional environments, primarily in that the time of burial was longer and temperature was lower. Diagenetic processes have had about 10 times as long to act on these Pennsylvanian sediments but at less than half the temperature of the diagenetic environment of the Cenozoic and Mesozoic sediments. The diagenetic transformation of the minerals in the Browning Sandstone occurred within a system that was more open than that of the Purington Shale, which is from 5 to 10 m above the Browning Sandsone in the same cyclothem (fig. 1).

The diagenetic changes recognized in the Browning Sandstone represent similar changes in all of the Paleozoic rocks of the Illinois Basin. These changes indicate that there were transfers of enormous amounts of material within, into, and out of the Illinois Basin. Understanding this large-scale, long-term process, which is still continuing, is essential to unraveling the geologic history of the Illinois Basin and its many economic and environmental applications.

ACKNOWLEDGMENTS

REFERENCES

Boles, J.R., 1982, Active albitization of plagioclase, Gulf Coast Tertiary: American Journal of Science, v. 282, p. 165–180.

Bostick, N.H., S.M. Cashman, T.H. McColloch, and C.T. Waddel, 1979, Gradients of vitrinite reflectance and present temperature in Los Angeles and Ventura Basins, California, in D.F. Oltz, ed., Low temperature metamorphism of kerogen and clay minerals: Pacific Section, Society for Sedimentary Geology, p. 65–96.

de Caritat, P., J.D. Bloch, I.E. Hutcheon, F.J. Longstaffe, and H.J. Abercrombie, 1997, Comparison of the mineralogical and chemical composition of two shales from the Western Canada Sedimentary Basin and the United States Gulf Coast: Clays and Clay Minerals, v. 45, p. 327–332.

Charles, R.G., and H. Blatt, 1978, Quartz, chert, and feldspars in modern fluvial muds and sands: Journal of Sedimentary Petrology, v. 48, p. 427–432.

Cluff, R.M., and A.P. Byrnes, 1990, Lopatin analysis of maturation and petroleum generation in the Illinois Basin, in M.W. Leighton, D.R. Kolata, D.F. Oltz, and J.J. Eidel, eds., Interior cratonic basins: Tulsa, Oklahoma, American Association of Petroleum Geologists, Memoir 51 (World Petroleum Basins), p. 425–437.

Damberger, H.H., 1991, Coalification in North American coal fields, in H.J. Gluskoter, D.D. Rice, and R.B. Taylor Jr., eds., Economic geology, U.S.—The geology of North America, Part 2: Boulder, Colorado, Geological Society of America, p. 503–522.

Deer, W.A., R.A. Howie, and J. Zussman, 1962, Rock forming minerals, vol. 3, Sheet silicates: New York, John Wiley & Sons, 270 p.

Frye, J.C., H.D. Glass, and H.B. Willman, 1962, Stratigraphy and mineralogy of the Wisconsinan loesses of Illinois: Illinois State Geological Survey, Circular 334, p. 55.

Gharrabi, M., and B. Velde, 1995, Clay mineral evolution in the Illinois Basin and its causes: Clay Minerals, v. 30, p. 353–364.

Gharrabi, M.B., B. Velde, and J.P. Sagon, 1998, The transformation of illite to muscovite in pelitic rocks—Constraints from x-ray diffraction: Clays and Clay Minerals, v. 46, p. 79–88.

Grathoff, G.H., 1996, Illite in the Lower Paleozoic of the Illinois Basin—Origin, age, and polytype quantification: unpublished Ph.D. thesis, University of Illinois at Urbana-Champaign, 87 p.

Grathoff, G.H., and D.M. Moore, 1996, Illite polytype quantification using WILDFIRE® calculated x-ray diffraction patterns: Clays and Clay Minerals, v. 44, p. 835–842.

Grathoff, G.H., D.M. Moore, R.L. Hay, and K. Wemmer, 1998, Illite polytype quantification and K/Ar dating of Paleozoic shales—A technique to quantify diagenetic and detrital illite, in J. Schieber, W. Zimmerle, and P. Sethi, eds., Shales and Mudstones II: E. Schweizerbart'sche Verlagsbuchhandlung (Nägele u. Obermiller), Stuttgart, Germany, p. 161–175.

Greb, S.F., D.A. Williams, and A.D. Williamson, 1992, Geology and stratigraphy of the Western Kentucky Coal Field: Lexington, Kentucky Geological Survey, Series XI, Bulletin 2, 77 p.

Guidotti, C.V., and F.P. Sassi, 1998, Petrogenetic significance of Na-K white mica mineralogy— Recent advances for metamorphic rocks: European Journal of Mineralogy, v. 10, p. 815–854.

Hacquebard, P.A., 1977, Rank of coal as an index of organic metamorphism for oil and gas in Alberta: Geological Survey of Canada, Bulletin 262, p. 11–22.

Harvey, R.D., J.C. Crelling, R.R. Dutcher, and J.A. Schleicher, 1977, Petrology and related chemistry of coals in the Illinois Basin, in J.E. Palmer, and R.R. Dutcher, eds., Depositional and structural history of the Pennsylvanian System of the Illinois Basin, Part 2: Invited papers, Illinois State Geological Survey, Guidebook Series 15a, p. 127–142.

Hower, J., and S.P. Altaner, 1983, The petrologic significance of illite/smectite (abs.): Buffalo, New York, Clay Minerals Society, 20th Annual Meeting, p. 40.

Hower, J., E.V. Eslinger, M.E. Hower, and E.A. Perry, 1976, Mechanism of burial metamorphism of argillaceous sediments: Geological Society of America Bulletin, v. 87, p. 725–737.

Hughes, R.E., D.M. Moore, and H.D. Glass, 1994, Qualitative and quantitative analysis of clay minerals in soils: in J.E. Amonette, and L.W. Zelazny, eds., Quantitative methods in soil mineralogy: Madison, Wisconsin, Soil Science Society of America, Special Publication 35, p. 330–359.

Kirsimäe, K., and P. Jørgensen, 2000, Mineralogical and Rb-Sr isotope studies of low-temperature diagenesis of Lower Cambrian clays of the Baltic Paleobasin of north Estonia: Clays and Clay Minerals, v. 48, p. 95–105.

Kirsimäe, K., P. Jørgensen, and V. Kalm, 1999, Low-temperature diagenetic illite-smectite in Lower Cambrian clays in North Estonia: Clay Minerals, v. 34, p. 151–163.

Land, L.S., L.E. Mack, K.L. Milliken, and F.L. Lynch, 1997, Burial diagenesis of argillaceous sediment, south Texas Gulf of Mexico sedimentary basin—A reexamination: Geological Society of America Bulletin, v. 109, p. 2–15.

Land, L.S., and K.L. Milliken, 1981, Feldspar diagenesis in the Frio Formation, Brazoria County, Texas Gulf Coast: Geology, v. 9, p. 314–318.

Lanson, B., and D. Champion, 1991, The I/S to illite reaction in the late stage of diagenesis: American Journal of Science, v. 291, p. 473–506.

Lanson, B., B. Velde, and A. Meunier, 1998, Late stage diagenesis of illitic clay minerals as seen by decomposition of x-ray diffraction patterns—Contrasted behaviors of sedimentary basins with different burial histories: Clays and Clay Minerals, v. 46, p. 69–78.

Laury, R.L., 1968, Sedimentology of the Pleasantview Sandstone, southern Iowa and western Illinois: Journal of Sedimentary Petrology, v. 38, 568–599.

Leighton, M.W., D.R. Kolata, D.F. Oltz, and J.J. Eidel, eds., 1990, Interior cratonic basins: Tulsa, Oklahoma, American Association of Petroleum Geologists, Memoir 51 (World Petroleum Basins), 819 p.

Lynch, F.L., 1997, Frio Shale mineralogy and the stoichiometry of the smectite-to-illite reaction—The most important reaction in clastic sedimentary diagenesis: Clays and Clay Minerals, v. 45, p. 618–631.

Meunier, A., and B. Velde, 1989, Solid solutions in I-S mixed layers and illite: American Mineralogist, v. 74, p. 1106–1112.

Milliken, K.L., 1988, Loss of provenance information through subsurface diagenesis in Plio-Pleistocene sandstones, northern Gulf of Mexico: Journal of Sedimentary Petrology, v. 58, p. 992–1002.

Milliken, K.L., 1992, Chemical behavior of detrital feldspars in mudrocks versus sandstones, Frio Formation (Oligocene), south Texas: Journal of Sedimentary Petrology, v. 62, p. 790–801.

Milliken, K.L., E.F. McBride, and L.S. Land, 1989, Numerical assessment of dissolution versus replacement in the subsurface destruction of detrital feldspars, Oligocene Frio Formation, south Texas: Journal of Sedimentary Petrology, v. 59, p. 740–757.

Moore, D.M., 1978, A sample of the Purington Shale prepared as a geochemical standard: Journal of Sedimentary Petrology, v. 48, p. 995–998.

Moore, D.M., 1982, Shallow burial diagenesis of the Pennsylvanian Purington Shale: Program with abstracts, 19th Annual Meeting, The Clay Minerals Society, p. 73.

Moore, D.M., 1984, Modal analysis and mineral chemistry of the Pennsylvanian Purington Shale: Lexington, Kentucky, Geological Society of America, Program with Abstracts, North-Central Meeting, v. 16, no. 3, p. 181.

Moore, D.M., 2000, Diagenesis of the Purington Shale in the Illinois Basin and implications for the diagenetic state of sedimentary rocks of shallow, Paleozoic basins: Journal of Geology, v. 108, p. 553–567.

Moore, D.M., and R.E. Hughes, 1991, Characteristics of chlorite interlayered with a 7Å mineral as found in sandstone reservoirs: Houston, Texas, Program with Abstracts, Annual Meeting of Clay Minerals Society, p. 115.

Moore, D.M., and R.C. Reynolds, Jr., 1997, X-ray diffraction and the identification and analysis of clay minerals, 2nd edition: New York, Oxford University Press, 378 p.

Newman, A.C.D., and G. Brown, 1987, The chemical constitution of clays: in A.C.D. Newman, ed., Chemistry of clays and clay minerals: New York, John Wiley & Sons, Mineralogical Society, Monograph No. 6, p. 1–128.

Perry, E.A., and J. Hower, 1970, Burial diagenesis in Gulf Coast pelitic sediments: Clays and Clay Minerals, v. 18, 165–177.

Pevear, D.R., 1992, Illite age analysis, a new tool for basin thermal history analysis, in Y.K. Kharaka, and A.S. Maest, eds., Water-rock interaction: Rotterdam, the Netherlands, A.A. Balkema, p. 1251–1254.

Pevear, D.R., 1999, Illite and hydrocarbon exploration: Proceedings of the National Academy of Sciences, v. 96, p. 3440–3446.

Potter, P.E., and H.D. Glass, 1958, Petrology and sedimentation of the Pennsylvanian sediments in southern Illinois—A vertical profile: Illinois State Geological Survey, Report of Investigations 204, 60 p.

Potter, P.E., and W.A. Pryor, 1961, Dispersal centers of Paleozoic and later clastics of the Upper Mississippi Valley and adjacent areas: Geological Society of America Bulletin, v. 72, p. 1195–1249.

Potter, P.E., and R. Siever, 1956, Sources of basal Pennsylvanian sediments in the Eastern Interior Basin 1—Cross-bedding: Journal of Geology, v. 64, p. 225–244.

Primmer, T.J., and H.F. Shaw, 1985, Diagenesis of shales: Evidence from backscattered electron microscopy and electron microprobe analyses, in L.G. Schultz, H. van Olphen, and F.A. Mumpton, eds., Proceedings of the International Clay Conference, p. 135–143.

Reynolds, R.C., Jr., 1985, NEWMOD* A computer program for the calculation of one-dimensional diffraction patterns of mixed-layered clays: Hanover, New Hampshire, R.C. Reynolds, Jr.

Rowan, E.L., and M.B. Goldhaber, 1996, Fluid inclusions and biomarkers in the Upper Mississippi Valley zinc-lead district—Implications for the fluid-flow and thermal history of the Illinois Basin: Washington, D.C., U.S. Geological Survey, Bulletin 2094-F, 34 p.

Ryan, P.C., M.E. Conrad, K. Brown, C.P. Chamberlain, and R.C. Reynolds, Jr., 1998, Oxygen isotope compositions of mixed-layer serpentine-chlorite and illite-smectite in the Tuscaloosa Formation (U.S. Gulf Coast)—Implications for pore fluids and mineralogic reactions: Clays and Clay Minerals, v. 46, p. 357–368.

Ryan, P.C., and R.C. Reynolds, Jr., 1996, The origin and diagenesis of grain-coating serpentine-chlorite in Tuscaloosa Formation sandstone, U.S. Gulf Coast: American Mineralogist, v. 81, p. 213–225.

Shau, Y.-H., M.E. Feather, E.J. Essene, and D.R. Peacor, 1991, Genesis and solvus relations of submicroscopically intergrown paragonite and phengite in a blue schist from northern California: Contributions to Mineralogy and Petrology, v. 106, p. 367–378.

Siever, R., and P.E. Potter, 1956, Sources of basal Pennsylvanian sediments in the Eastern Interior Basin 2—Sedimentary petrology: Journal of Geology, v. 64, p. 317–335.

Srodoń, J., F. Elass, W.J. McHardy, and D.J. Morgan, 1992, Chemistry of illite-smectite inferred from TEM measurements of fundamental particles: Clay Minerals, v. 27, p. 137–58.

Trevena, A.S., and W.P. Nash, 1979, Chemistry and provenance of detrital plagioclase: Geology, v. 7, p. 475–478.

Treworgy, C.G., and R.J. Jacobson, 1985, Paleoenvironments and distribution of low-sulfur coal in Illinois, in A.T. Cross, ed., Economic geology; Coal, oil and gas, v. 4, Compte Rendu, Ninth International Congress on Carboniferous Stratigraphy and Geology: Carbondale, Illinois, Southern Illinois University Press, p. 349–359.

Wanless, H.R., 1957, Geology and mineral resources of the Beardstown, Glasford, Havana, and Vermont Quadrangles: Illinois State Geological Survey, Bulletin 82, 233 p.

Willman, H.B., E. Atherton, T.C. Buschbach, C. Collinson, J.C. Frye, M.E. Hopkins, J.A. Lineback, and J.A. Simon, 1975, Handbook of Illinois stratigraphy: Illinois State Geological Survey, Bulletin 95, 261 p.

Wright, C.R., 1966, Environmental mapping of the beds of the Liverpool Cyclothem in the Illinois Basin and equivalent strata in the northern mid-continent region: unpublished Ph.D. thesis, University of Illinois at Urbana-Champaign, 99 p.

Depatment of Natural Resources
ILLINOIS STATE GEOLOGICAL SURVEY
Natural Resources Building
615 East Peabody Drive
Champaign, IL 61820-6964